

Article

Prediction of Splitting Tensile Strength of Self-Compacting Recycled Aggregate Concrete Using Novel Deep Learning Methods

Jesús de-Prado-Gil ^{1,*}, Osama Zaid ², Covadonga Palencia ¹ and Rebeca Martínez-García ³

¹ Department of Applied Physics, Campus of Vegazana s/n, University of León, 24071 León, Spain; c.palencia@unileon.es

² Department of Structure Engineering, Military College of Engineering, Risalpur, National University of Sciences and Technology, Islamabad 44000, Pakistan; Osama.zaid@scetwah.edu.pk

³ Department of Mining Technology, Topography and Structures, Campus de Vegazana s/n, University of León, 24071 León, Spain; rmartg@unileon.es

* Correspondence: jdeprg00@estudiantes.unileon.es

Abstract: The composition of self-compacting concrete (SCC) contains 60–70% coarse and fine aggregates, which are replaced by construction waste, such as recycled aggregates (RA). However, the complexity of its structure requires a time-consuming mixed design. Currently, many researchers are studying the prediction of concrete properties using soft computing techniques, which will eventually reduce environmental degradation and other material waste. There have been very limited and contradicting studies regarding prediction using different ANN algorithms. This paper aimed to predict the 28-day splitting tensile strength of SCC with RA using the artificial neural network technique by comparing the following algorithms: Levenberg–Marquardt (LM), Bayesian regularization (BR), and Scaled Conjugate Gradient Backpropagation (SCGB). There have been very limited and contradicting studies regarding prediction by using and comparing different ANN algorithms, so a total of 381 samples were collected from various published journals. The input variables were cement, admixture, water, fine and coarse aggregates, and superplasticizer; the data were randomly divided into three sets—training (60%), validation (10%), and testing (30%)—with 10 neurons in the hidden layer. The models were evaluated by the mean squared error (MSE) and correlation coefficient (R). The results indicated that all three models have optimal accuracy; still, BR gave the best performance ($R = 0.91$ and $MSE = 0.2087$) compared with LM and SCG. BR was the best model for predicting TS at 28 days for SCC with RA. The sensitivity analysis indicated that cement (30.07%) was the variable that contributed the most to the prediction of TS at 28 days for SCC with RA, and water (2.39%) contributed the least.

Keywords: artificial neural network; self-compacting concrete; recycled aggregates; tensile strength; Levenberg–Marquardt; Bayesian regularization; scaled conjugate gradient backpropagation

MSC: 68T07



Citation: de-Prado-Gil, J.; Zaid, O.; Palencia, C.; Martínez-García, R. Prediction of Splitting Tensile Strength of Self-Compacting Recycled Aggregate Concrete Using Novel Deep Learning Methods. *Mathematics* **2022**, *10*, 2245. <https://doi.org/10.3390/math10132245>

Academic Editors: Araceli Queiruga-Dios, Maria Jesus Santos, Fatih Yilmaz, Deolinda M. L. Dias Rasteiro, Jesús Martín Vaquero and Víctor Gayoso Martínez

Received: 14 June 2022

Accepted: 24 June 2022

Published: 27 June 2022

Publisher's Note: MDPI stays neutral with regard to jurisdictional claims in published maps and institutional affiliations.



Copyright: © 2022 by the authors. Licensee MDPI, Basel, Switzerland. This article is an open access article distributed under the terms and conditions of the Creative Commons Attribution (CC BY) license (<https://creativecommons.org/licenses/by/4.0/>).

1. Introduction

Concrete is the most widely used construction material in the world. One of the main arduous tasks is to produce durable concrete without excessive voids and with a long service life [1]. Due to extensive research, concrete design technology has improved in past years by adding certain admixtures [2,3]. Self-compacting concrete, created in Japan in the 1980s to achieve high-performance, long-lasting concrete buildings, is one of the outcomes of improved concrete design technology [4–6]. The main distinction between self-compacting concrete and conventional concrete is the mixing proportions of the materials [7–9]. SCC is known as the innovative concrete of the era and has the property

of self-settlement in construction areas without vibratory force. SCC settles under its weight by making its path like fluid [10–12]. SCC is considered innovative because it can easily be used in congested areas where concreting is not easy. In SCC, noise pollution reduces and improves the filling capability and enhances the construction speed [13–15]. The population is growing at an alarming rate worldwide, along with the adoption and implementation of new concrete design technologies, resulting in increased resource consumption and environmental degradation. In consequence, there has been an increase in the amount of building and construction waste [16,17]. In terms of the composition of concrete, coarse aggregate (natural crushed stone) and fine aggregate (sand) make up most of the self-compacting concrete, approximately 60–70% [18–20]. Simultaneously, natural resources are being depleted at a high speed due to modern urbanization [21–23]. The primary source of well-quality aggregates, i.e., mountains, are being depleted at an alarming rate [24–26]. Because of this, natural catastrophes have struck many countries worldwide [27–29]. On the other hand, many buildings are demolished yearly due to earthquakes or after completing their service life [19,27,30]. Therefore, a considerable amount of construction waste is generated annually. To counter such things, the most sustainable revolution is to use recycled aggregates in self-compacting concrete. Recycled aggregates (RA) are abundant waste products developed by demolishing the building and then crushing, sieving, and adequately cleaning [31]. The second procedure is to bypass all these experimental works, thus reducing environmental degradation and other wastage of natural materials.

Currently, many researchers are working on using soft computing techniques. One such method is using an artificial neural network (ANN) to validate and predict specific parameters of concrete. The artificial neural network technique is generally motivated by the human brain, which is composed of billions of neurons. The ANN works similarly, learning from experiences and then utilizing the data to predict different parameters [32,33].

2. Background Literature

2.1. Artificial Neural Network

Artificial neural networks (ANNs) are a fundamental technique in deep learning. Deep learning (DL) is a subset of machine learning (ML) that allows for the computation of multi-layer neural networks. Machine learning is a subset of artificial intelligence (AI) that uses statistical methods to enable computers to develop over time, unlike the primary subject of AI, which allows machines to mimic human behavior. The primary difference between ML and DL is that in deep learning, the machine performs feature extraction and classification. Still, in machine learning, we must perform the feature extraction ourselves, and the machine performs the classification and prediction [34].

An artificial neural network (ANN) is a mathematical or computer model inspired by the human brain's enormous biological neural network [35]. It can improve its performance by learning from its mistakes, which is how an artificial neural network receives information, i.e., by learning. It comprises several functions and weights that operate as artificial neurons and are connected in a network. They are primarily used in artificial intelligence projects that solve complicated and complex issues [32]. ANN can be operated using specific algorithms that are unique in their way. From this paper's point of view, LM, BR, and SCGB are discussed below.

2.1.1. Levenberg–Marquardt Algorithm

The Levenberg–Marquardt (LM) algorithm is a procedure composed of several iterations. These iterations are used to find the minimum value of a multivariate function written as the sum of squares of non-linear real-valued functions [36,37]. Researchers recently adopted this approach to solve nonlinear least square complex problems across a wide range of fields [38]. In the LM algorithm, two methods are combined to speed up the iterations and minimize errors, i.e., the steepest descent and the Gauss–Newton method. When the present outcome is correct, the algorithm becomes the Gauss–Newton method faster than another. When the outcome is incorrect, it behaves like the steepest descent,

which is relatively slow but always converges [39]. This algorithm generally uses more memory but less time.

2.1.2. Bayesian Regularization

Standard backpropagation nets are less reliable than Bayesian regularized artificial neural networks (BRANNs), which can decrease or eliminate the requirement for prolonged cross-validation [40]. In the same way that ridge regression makes a nonlinear regression into a “well-posed” statistical issue, Bayesian regularization does the same for nonlinear regression. It takes more time, but the model has numerous benefits over complex data [41]. The advantage of using BRANNs is that the models are reliable, and a validation procedure is not required [40,42]. These networks address various issues that emerge in Quantitative Structure–Activity Relationship (QSAR) modeling, including model selection, robustness, validation set selection, and network architectural optimization [43]. Bayesian criteria are stopped during training by empirical processes, making the network impossible to over train.

2.1.3. Scaled Conjugate Gradient Backpropagation

The weights are attuned in the steepest descent direction, i.e., the most negative of the gradients, via the fundamental backpropagation method. This is the fastest reducing path for the performance function. It is noted that while the function reduces the quickest along with the negative of the gradient, this does not lead to the fastest convergence [44].

The conjugate gradient algorithms search in a path that generally yields quicker convergence than the sharpest descent direction while sustaining the error reduction made in the previous phases [45]. The conjugate direction is the name given to this direction. The step size is modified in most conjugate gradient algorithms through each iteration. A search is conducted along the conjugate gradient direction to calculate the step size that will lessen the performance function along the line [46]. It is also reasonable to approximate the step size using a method other than the line search methodology. The goal is to merge the Levenberg algorithm’s model trust region method with the conjugate gradient technique. SCG is the name given to this method, which was first described in the literature by Møller (1993) [47]. At every iteration user, design parameters are updated independently, which is critical for the algorithm’s success. This is an essential benefit of line search-based algorithms [47].

3. Research Significance

This research aimed to validate and predict the splitting tensile strength of self-compacting concrete incorporated with recycled aggregates by artificial neural networks. From the author’s best information related to the present literature, no significant studies have been conducted on applying different deep learning methods to predict the split tensile strength of SCC with RA. For this purpose, different algorithms were implemented, namely Levenberg–Marquardt (LM), Bayesian regularization (BR), and Scaled Conjugate Gradient Backpropagation (SCGB) algorithms. The best model was selected after comparing them using statistical indicators: correlation coefficient (R-value) and mean squared error (MSE). In the end, sensitivity analysis was performed to see how each input variable affected the output variable.

4. Methodology

4.1. Data Collection

The data were collected from various research articles. Table 1 shows the database containing a total of 381 samples comprised of the tensile strength of self-compacting concrete with recycled aggregates with several variables, such as water, cement, admixtures, coarse aggregates, water, fine aggregates, and superplasticizers. The database includes the Sr No., indicating the total number of research papers, authors’ references, amount of data (# data) contributing from each article, and percentage (% data) of the overall data.

Table 1. Experimental database.

No.	Reference	# Data	% Data	No.	Reference	# Data	% Data
1	Ali et al., 2012 [48]	18	4.72	22	Nieto et al., 2019 [49]	22	5.77
2	Aslani et al., 2018 [50]	15	3.94	23	Nili et al., [51]	10	2.62
3	Babalola et al., 2020 [52]	14	3.67	24	Pan et al., 2019 [53]	6	1.57
4	Bahrami et al., 2020 [54]	10	2.62	25	Revathi et al., 2013 [55]	5	1.31
5	Behera et al., 2019 [56]	6	1.57	26	Revilla Cuesta et al., 2020 [57]	5	1.31
6	Chakkamalayath et al., 2020 [58]	6	1.57	27	Sadeghi-Nik et al., 2019 [59]	12	3.15
7	Duan et al., 2020 [60]	10	2.62	28	Señas et al., 2016 [61]	6	1.57
8	Fiol et al., 2018 [62]	12	3.15	29	Sharific et al., 2013 [63]	6	1.57
9	Gesoglu et al., 2015 [64]	24	6.30	30	Khafaga, S.A., 2014 [65]	15	3.94
10	Grdic et al., 2010 [66]	3	0.79	31	Silva et al., 2016 [67]	5	1.31
11	Guneyisi et al., 2014 [68]	5	1.31	32	Singh et al., 2019 [69]	12	3.15
12	Guo et al., 2020 [70]	11	2.89	33	Sun et al., 2020 [71]	10	2.62
13	Katar et al., 2021 [72]	4	1.05	34	Surendar et al., 2021 [73]	7	1.84
14	Khodair et al., 2017 [74]	20	5.25	35	Tang et al., 2016 [75]	5	1.31
15	Kou et al., 2009 [76]	13	3.41	36	Thomas et al., 2016 [77]	4	1.05
16	Krishna et al., 2018 [78]	5	1.31	37	Tuyan et al., 2014 [79]	12	3.15
17	Kumar et al., 2017 [80]	4	1.05	38	Uygunoglu et al., 2014 [81]	8	2.10
18	Long et al., 2016 [82]	4	1.05	39	Wang et al., 2020 [83]	5	1.31
19	Mahakavi and Chitra, 2019 [84]	25	6.56	40	Yu et al., 2014 [85]	3	0.79
20	Manzi et al., 2017 [86]	4	1.05	41	Zhou et al., 2013 [87]	6	1.57
21	Martínez-García et al., 2020 [88]	4	1.05		Total	381	100

Table 2 presents the statistical characteristics, such as the minimum, maximum, mean, median, mode, and standard deviation, of certain variables as inputs (water, cement, admixtures, coarse aggregates, water, fine aggregates, and superplasticizers) and one possible output from these published research articles, i.e., the tensile strength of self-compacting recycled aggregate concrete. Their graphical representation is shown in Figures 1 and 2.

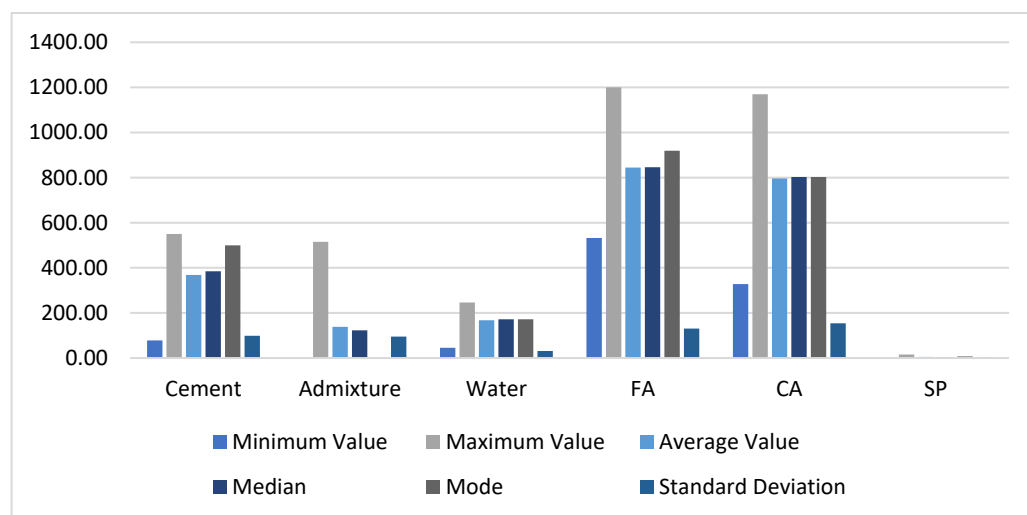


Figure 1. Statistical characteristics of input variables.

4.2. Data Visualization

The correlation between the input variables—i.e., water, cement, admixtures, coarse aggregates, water, fine aggregates, and superplasticizers—and output—i.e., splitting tensile strength (TS)—was investigated to see whether there was a link between them; this statistical analysis assisted in the creation of the predictive model by increasing the accuracy of the outcome’s prediction [89]. For this purpose, the Pearson correlation matrix (heat map) was generated, as shown in Figure 3, which analyzed the correlation between the independent input variables. A correlation ($|r| > 0.8$) between input variables might indicate that there

is currently multicollinearity between variables, which could alter modeling findings and bias the model. As seen in the heat map, although there was a substantial connection between some of the characteristics, such as between admixtures and cement ($r = -0.608$) and between coarse aggregates and fine aggregates ($r = -0.685$), none of the characteristics had a correlation greater than 0.80, showing that multicollinearity did not occur [90,91].

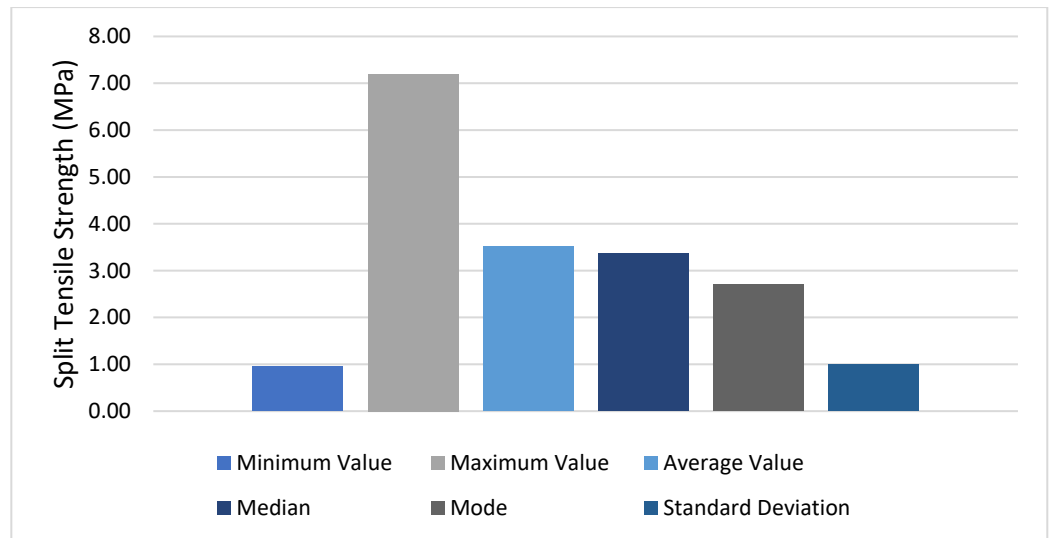


Figure 2. Statistical characteristics of the output variable.

Table 2. Statistical characteristics of input and output variables.

	Variables	Abbreviation	Minimum	Mean	Maximum	Median	Mode	Standard Deviation
Input (kg/m ³)	Cement	C	78.00	368.73	550.00	385.00	500.00	98.38
	Admixture	A	0.00	138.27	515.00	123.00	0.00	94.95
	Water	W	45.50	167.29	246.00	172.00	172.00	31.02
	Fine Aggregates	FA	532.20	844.71	1200.00	846.00	919.00	130.52
	Coarse Aggregates	CA	328.00	196.05	1170.00	803.00	803.00	154.06
Output (MPa)	Super Plasticizer	SP	0.00	5.07	16.00	4.55	7.50	3.12
	Tensile Strength	TS	0.96	3.52	7.20	3.37	2.70	1.00

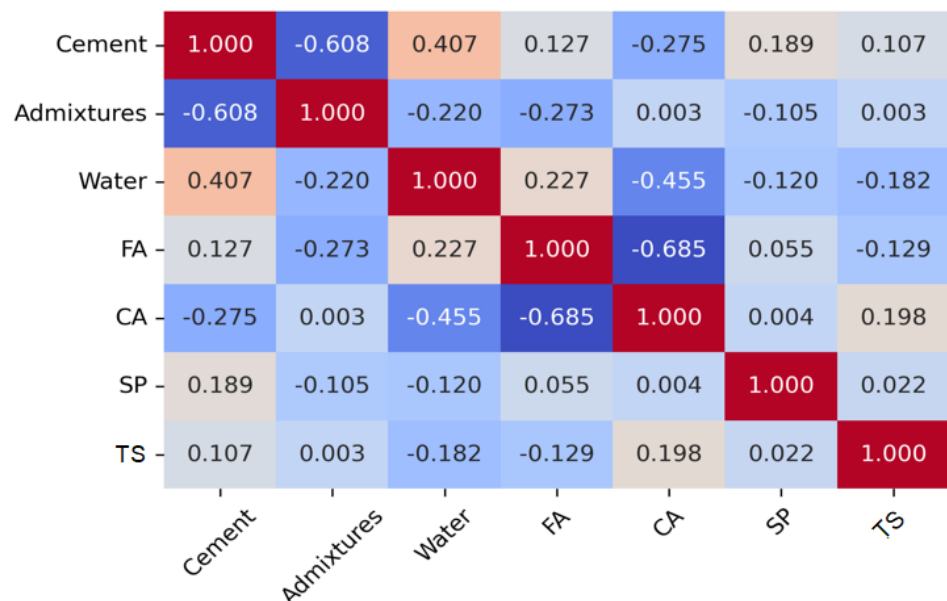


Figure 3. Correlation coefficient heat map between the input and output variables.

4.3. Artificial Neural Network for the Training, Validation, and Prediction of the Tensile Strength

An artificial neural network (ANN) is a mathematical or computational model influenced by biological neural networks' structural and/or functional characteristics. It can improve its performance by learning from its mistakes. Artificial neural networks, like human brains, acquire knowledge through learning. They are made up of a network of artificial neurons that communicate with one another and analyze data using a connectionist approach to computation. They are primarily employed to simulate complicated input–output interactions or data patterns in data [14]. Training, validation, and testing are the three phases of ANNs. The model is repeated until it reaches the desired outcome in the training phase. The validation step's mistakes are detected during the training phase [92].

An ANN model generally comprises several layers, the first of which is input and output, which contains input and output data. Depending on the model, one or more hidden layers exist between these layers. It is made up of neurons that are linked by weights. The output of each neuron is determined by its activation function. Activation functions come in several different forms. Nonlinear activation functions, such as sigmoid and step, are commonly employed [1]. The general structure of an ANN is shown in Figure 4.

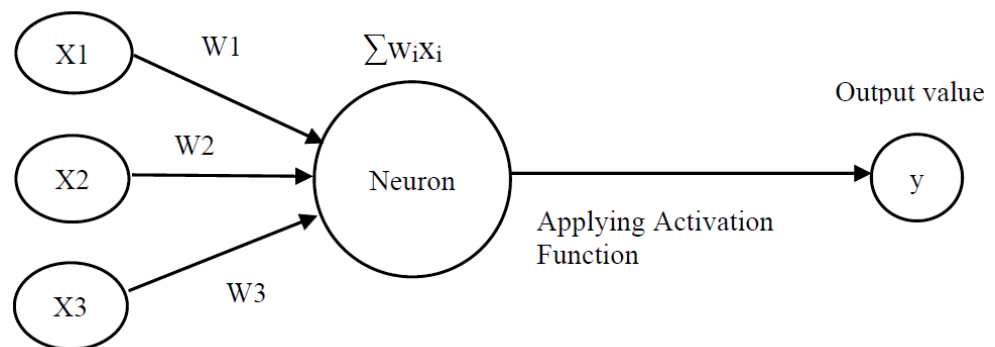


Figure 4. General structure of ANN.

A variety of factors must be considered while creating an ANN model. The first step is selecting the most appropriate structure for the ANN model. Then, the data are inserted into the selected ANN model in terms of input and output. Then, in the activation function, the number of layers and the number of hidden layers, as well as some neurons in each hidden layer, must be selected by experience [93,94].

In this research, concerning Tables 1 and 2, the network was made utilizing six input parameters and one output parameter with one hidden layer. The input layer consists of variables such as cement, admixtures, water, fine and coarse aggregates, and superplasticizer. The output parameter was selected by splitting the tensile strength of self-compacting recycled aggregate concrete. The feedforward backpropagation neural network was used in this study. The architecture of the current research on ANN is shown in Figure 5.

It should be noted that three algorithms were used and compared in this study, namely Levenberg–Marquardt (LM), Bayesian regularization (BR), and Scaled Conjugate Gradient backpropagation (SCG). Designing and performing the network were performed on MATLAB software. The Levenberg–Marquardt algorithm usually necessitates more memory, but it takes less time. Training terminates when generalization stops improving, as demonstrated by an increase in the mean square error of the validation samples. But in the case of Bayesian regularization, although this technique takes longer, it can provide strong generalization for complex, tiny, or noisy datasets. Adaptive weight reduction causes training to come to an end (regularization). On the other hand, the Scaled Conjugate Gradient Backpropagation algorithm uses less memory than the previous one. Training automatically terminates when generalization stops improving, as shown by a rise in the mean square error of the validation sample [45,46,94,95].

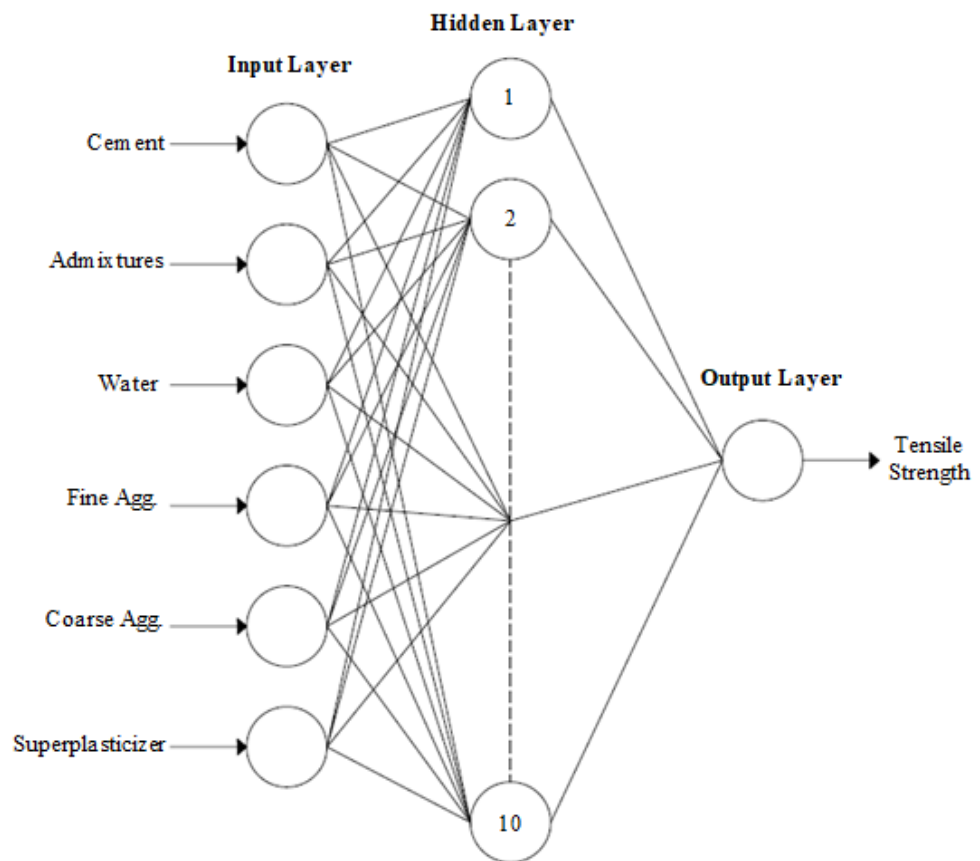


Figure 5. Artificial neural network architecture.

The models were developed and performed in MATLAB. The network was divided into three phases, i.e., training, validation, and testing. Sixty percent of data was selected for training, and the remaining 10% and 30% of data were selected for the validation and testing stage, respectively. In the training stage, 10 neurons were selected for the hidden layer. The network randomly chose data for training, validation, and testing according to its selected percentage, with 229 samples for training, 38 samples for validation, and 114 samples for the testing stage. In the case of Bayesian regularization (BR), validation is not required, so the numbers of samples taken for training and testing were 267 and 114, respectively. This is because validation is often employed as a type of regularization, while BR algorithms have their built-in form of validation. The splitting of data is summarized in Table 3.

4.4. ANN Network Model Evaluation

Using the ANN tool to develop the neural network; the models' performance was assessed using two measures; coefficient of correlation (R-value) and mean squared error (MSE) [96,97], as given in Equation (1).

$$\text{MSE} = \frac{1}{n} \sum (y_i - \hat{y}_i)^2 \quad (1)$$

where n = number of data points, y_i = observed values, and \hat{y}_i = predicted values.

Regression is considered the best evaluation measurement to check the accuracy of the overall network. The correlation between outputs and predicted targets was measured using R-values. A strong relationship has an R-value of 1, whereas a random relationship has an R-value of 0 [48,96].

The average squared discrepancy between outputs and objectives is known as the mean squared error. The lower the value, the better. There is no error if the value is zero.

Table 3. Data split for model testing.

Step	Percentage %	No. of Specimens
Levenberg–Marquardt Algorithm		
Train	60	229
Validation	10	38
Test	30	114
Total	100	381
Bayesian Regularization		
Train	70	267
Validation	-	0
Test	30	114
Total	100	381
Scaled Conjugate Gradient Backpropagation		
Train	60	229
Validation	10	38
Test	30	114
Total	100	381

5. Results and Discussion

The model was run on the basis of three algorithms, namely LM, BR, and SCG, separately, and their results are compared and discussed below.

5.1. Levenberg–Marquardt Algorithm

The network was trained again and again to find the best-fit model. The performance of the model is shown in Figure 6 with 10 neurons. The plot contains different colored lines indicating training, validation, and testing. The model started training with a high MSE, which was eventually reduced by the validation parameters preventing overfitting data. It shows that after 44 epochs, the training error was still decreasing, but the validation and testing errors were increasing. Therefore, after six more epochs, the model training was stopped, and an optimized model was produced with minimum MSE.

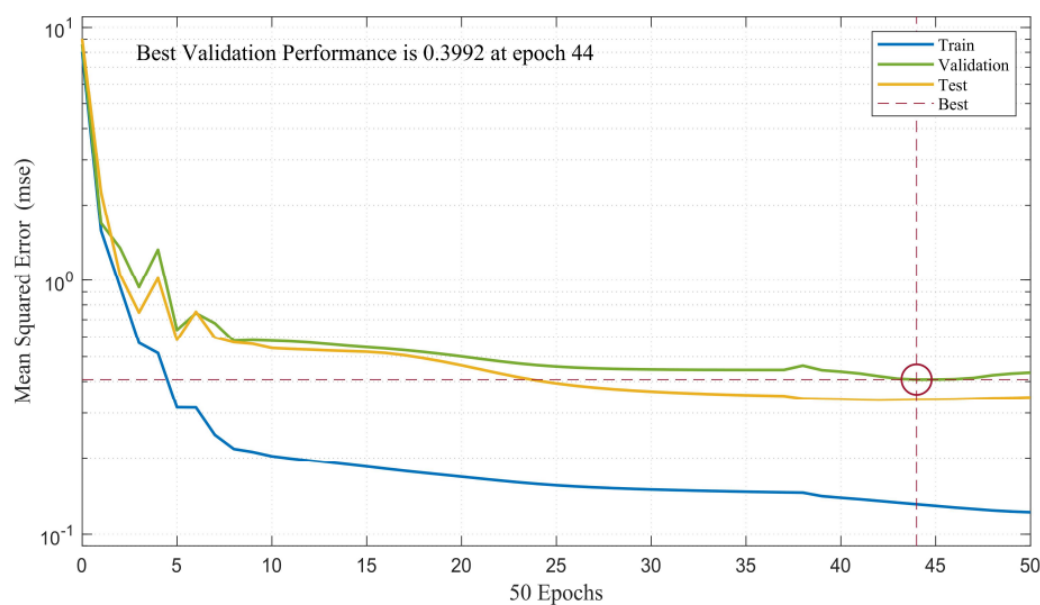


Figure 6. LM algorithm model performance.

The model error histogram is shown in Figure 7 between training, validation, and testing. The graph shows that the error bars converge to the zero-error line. The performance

criteria results show that the model is suitable for predicting the outcomes of splitting tensile strength of SCC with RA.

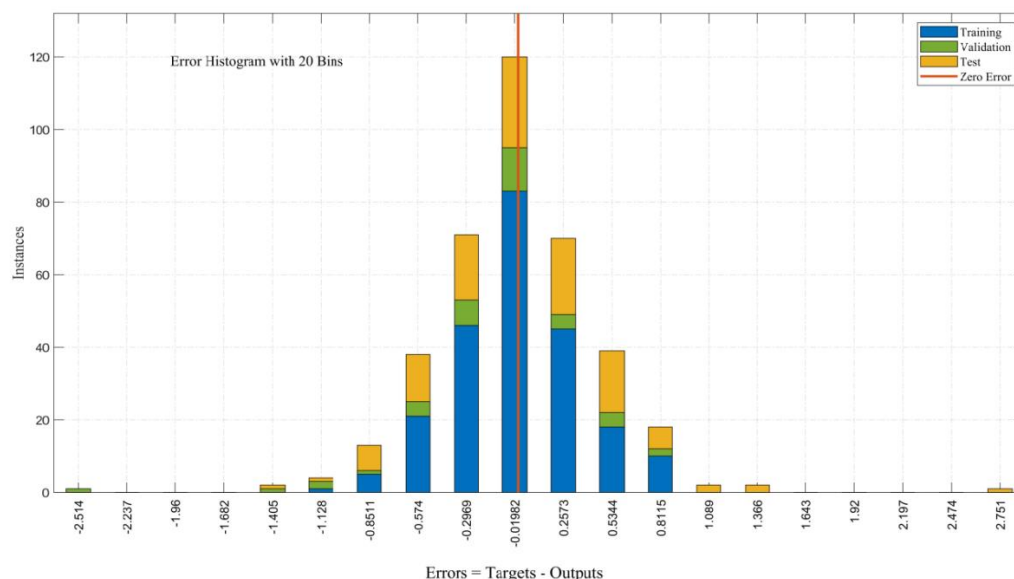


Figure 7. LM algorithm model error histogram.

After that, a regression analysis was performed. Figure 8a–c shows the correlation of training, validation, and testing between the input and output values of the model. The model’s overall accuracy, i.e., correlation, is shown in Figure 8d. In each scenario, a black-colored linear fit is displayed. It should be noted that the overall R-value was found to be 0.86, which shows that the correlation was very close to a linear fit, confirming a good model for predicting values of the splitting tensile strength of SCC using RA. Finally, all the performance parameters results, i.e., the R-value and MSE of the overall model with training, validation, and testing, are summarized in Table 4. Overall, these results indicate that the Levenberg–Marquardt algorithm is a good algorithm for predicting the splitting tensile strength of self-compacting recycled aggregate concrete.

Table 4. Summary of different model evaluation parameters of LM Algorithm.

Step	Function	MSE	R
Training	trainlm	0.1508	0.9267
Validation	trainlm	0.3992	0.7899
Testing	trainlm	0.3282	0.8294
Overall	trainlm	0.2927	0.8573

5.2. Bayesian Regularization

In the same manner, the model was trained using the Bayesian regularization approach. The model’s performance is shown in Figure 9 with the same number of neurons. The plot consists of two colored lines indicating training and testing only, as BR does not need a validation step because it has a built-in form of validation in the training step. The model started training with high MSE, which was eventually reduced by the training parameters preventing overfitting data. As BR takes more time, the graph shows that the model took several epochs, and after 100 epochs, training and testing error lines were reduced considerably and approximately became a straight line. The model is trained further to validate thoroughly, and training is stopped at 190 epochs. An optimized model has a 0.14403 performance indicator at 189 epochs.

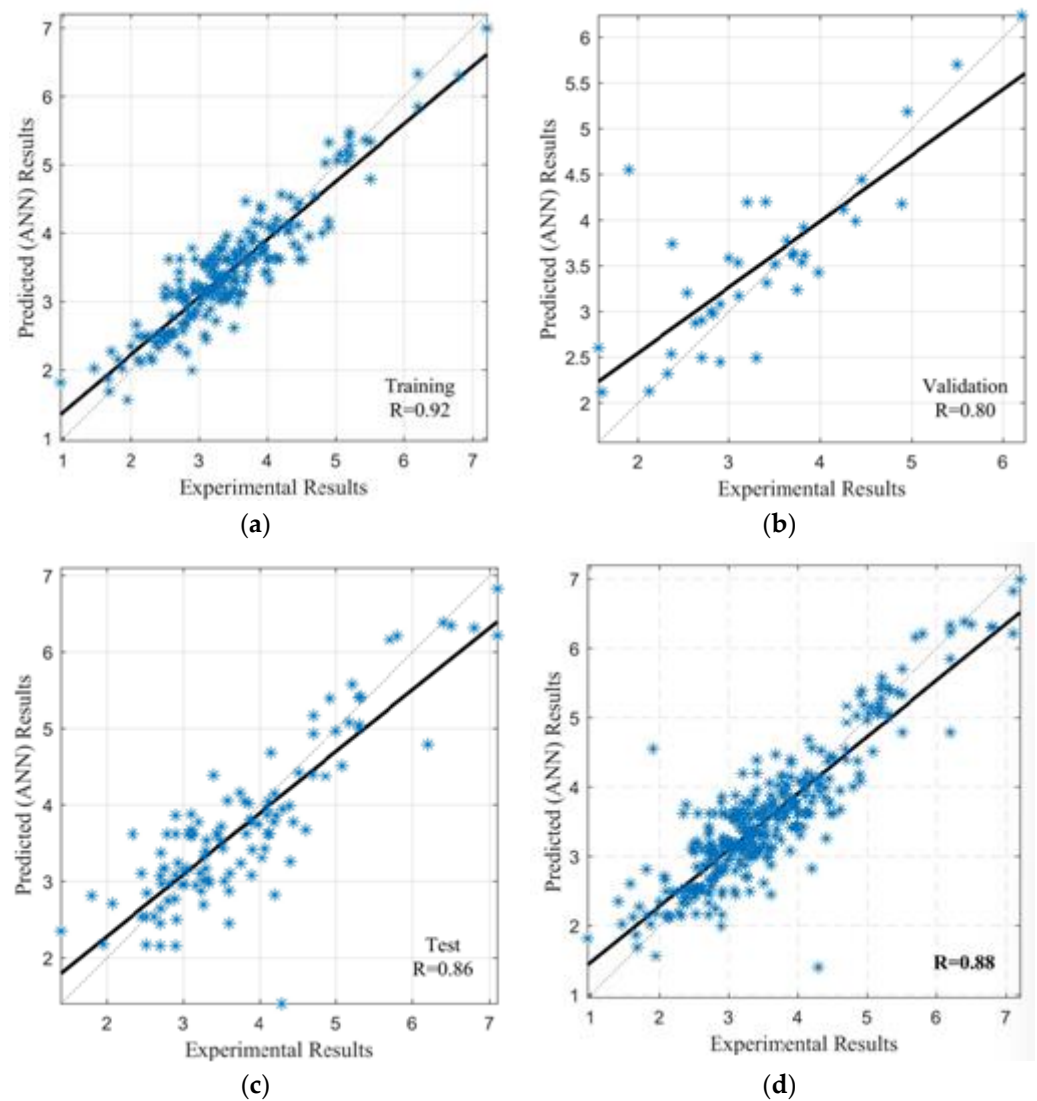


Figure 8. LM algorithm regression graphs between the experimental and predicted tensile strength: (a) training; (b) validation; (c) testing, and (d) overall dataset.

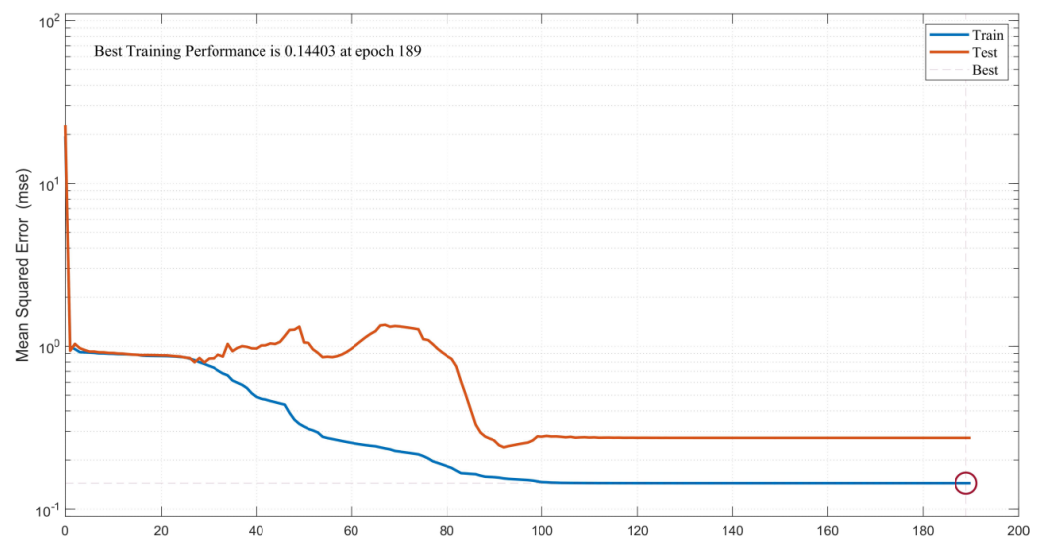


Figure 9. BR model performance.

The model error histogram is shown in Figure 10 between training and testing. The graph shows that the bins convergence to the zero-error line is excellent, and the error is also small compared to the LM algorithm. The results of this performance criteria are shown that the model is perfect for predicting the outcomes of splitting tensile strength of SCC with RA. After that, a regression analysis is performed in the same manner. Figure 11a,b show the correlation of training and testing between the input and output values of the model. Overall correlation is shown in Figure 11c. In each scenario, a black-colored linear fit is displayed. It is noted that the overall R-value is found to be 0.91. The model trained by Bayesian regularization has excellent accuracy for predicting output, i.e., splitting tensile strength of SCC with RA. Finally, all the performance parameters results, i.e., R-value and MSE of the overall model with training and test, are summarized in Table 5. Overall, these results indicate that Bayesian regularization can be adopted for predicting the splitting tensile strength of self-compacting recycled aggregate concrete.

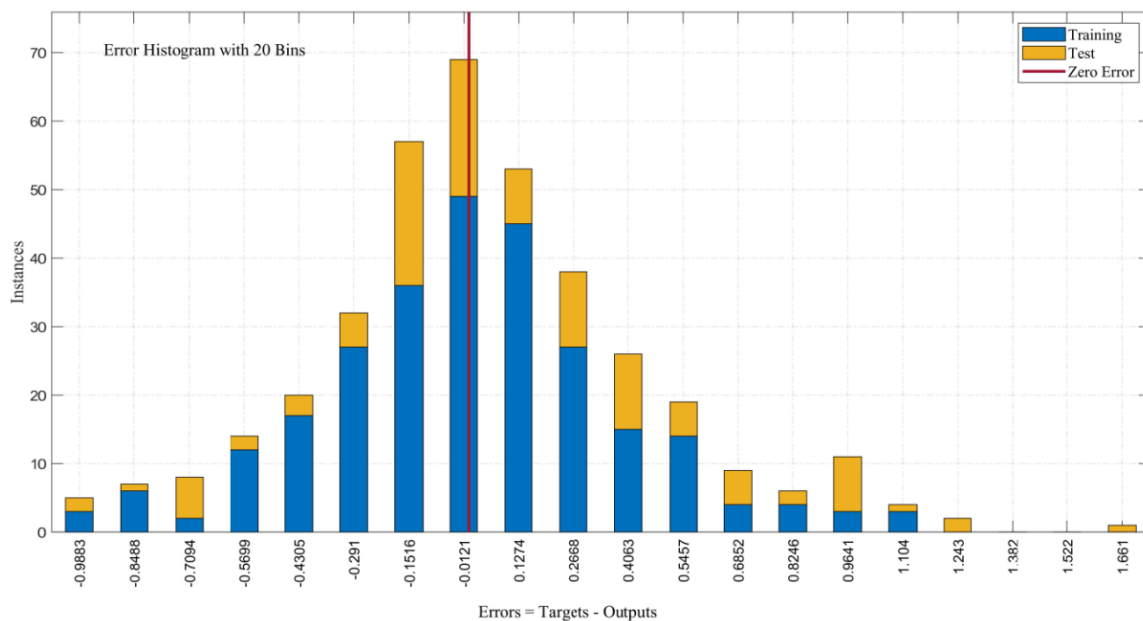


Figure 10. BR model error histogram.

Table 5. Summary of different model evaluation parameters of BR.

Step	Function	MSE	R
Training	trainbr	0.1440	0.9254
Testing	trainbr	0.2734	0.8638
Overall	trainbr	0.2087	0.9049

5.3. Scaled Conjugate Gradient Backpropagation

The model is trained by using the Scaled Conjugate Gradient Backpropagation approach. The performance of the model is shown in Figure 12 with 10 neurons. The plot contains different color lines indicating training, validation, and testing. The model starts training with high MSE, which is eventually reduced by the validation parameters preventing overfitting data. The graph shows that MSE did not reduce much compared with the other two algorithms. It shows that after 66 epochs, the training errors were decreasing, but the validation and testing errors were increasing a little bit. Therefore, after eight more epochs, the model training was stopped, and an optimized model was produced, with a minimum MSE achieved.

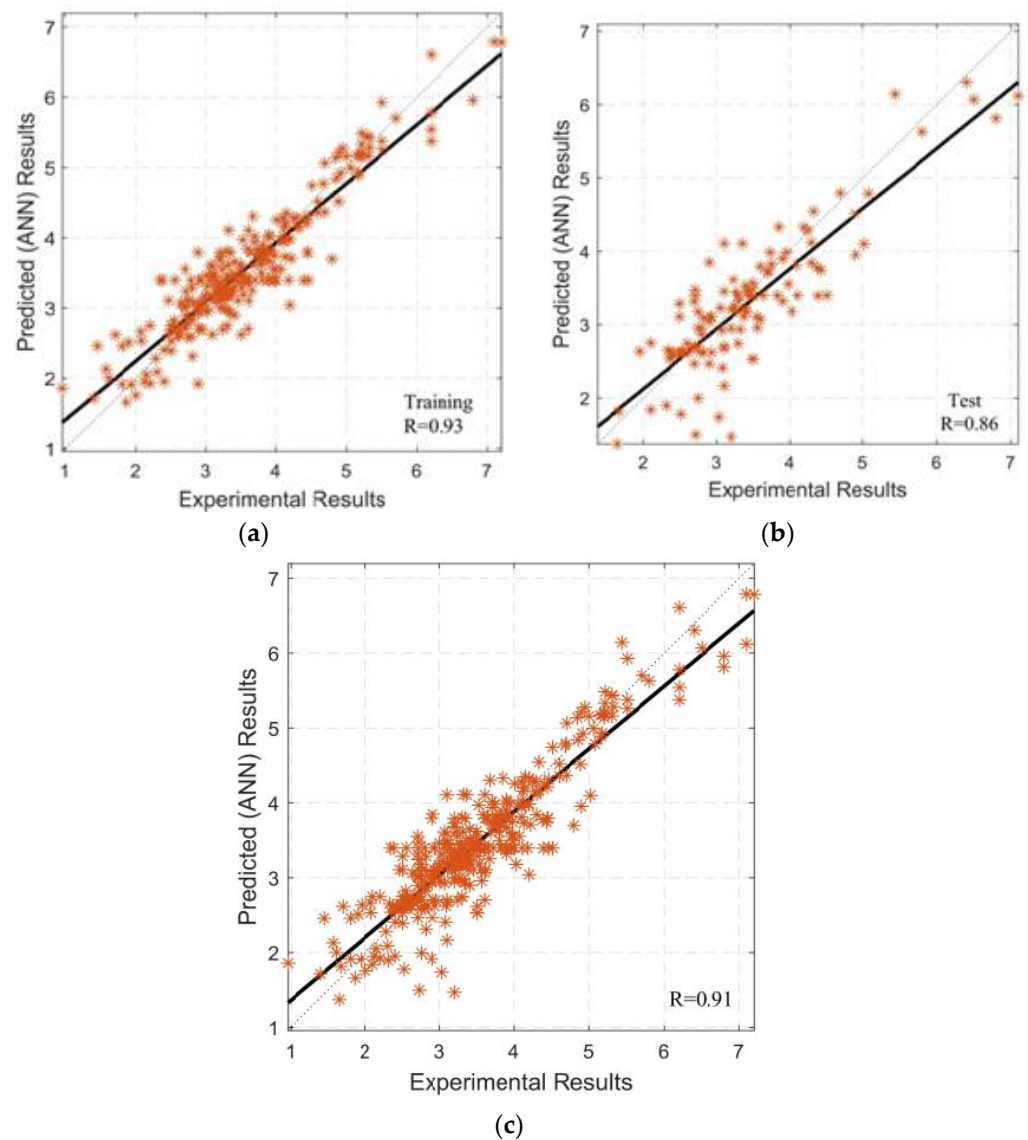


Figure 11. Bayesian regularization regression graphs between the experimental and predicted tensile strength: (a) training, (b) testing, and (c) overall dataset.

The model error histogram is shown in Figure 13 between training, validation, and testing. The graph shows that the error bar bins converge to the zero-error line with low accuracy. The results of this performance criteria indicate that the model has high error values compared with other algorithms and is below par for predicting the outcomes of splitting tensile strength of SCC with RA. After that, a regression analysis was performed. Figure 14a–c show the correlation of training, validation, and testing between the input and output values of the model. The model’s overall accuracy, i.e., correlation, is shown in Figure 14d. In each scenario, a maroon-colored linear fit is displayed. It should be noted that the overall R-value was found to be 0.64, which shows that the correlation was far from a linear fit, confirming a below-par or average model for predicting values of splitting tensile strength of SCC using RA.

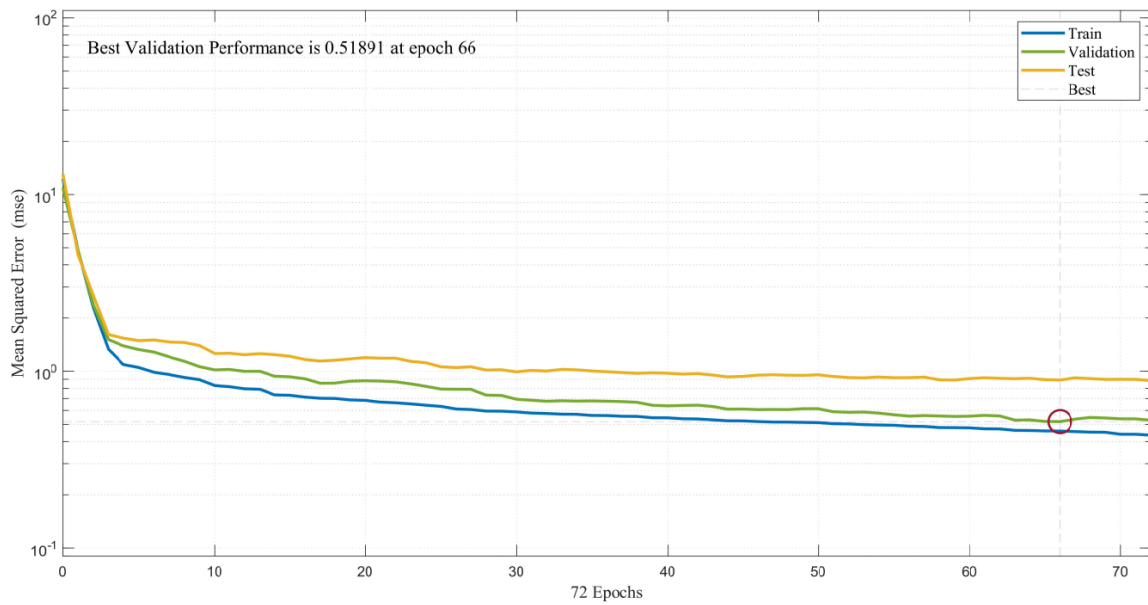


Figure 12. SCG model performance.

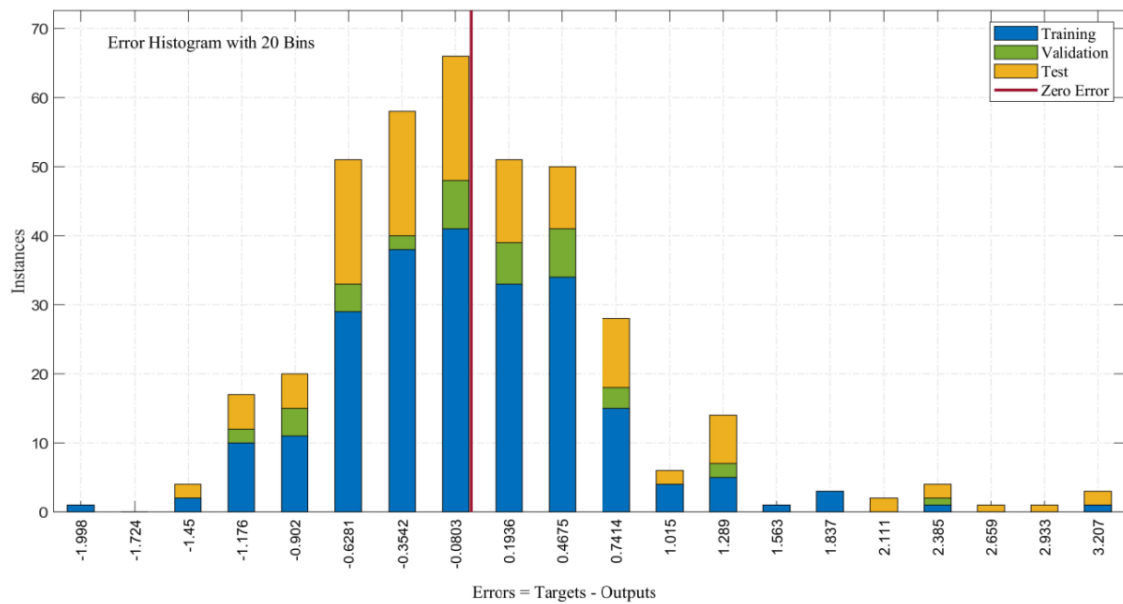


Figure 13. BR model error histogram.

Finally, all the performance parameters results, i.e., the R-value and MSE of the overall model with training, validation, and testing, are summarized in Table 6. These results indicate that Scaled Conjugate Gradient Backpropagation is rated as a below-par algorithm compared with LM and BR for predicting the splitting tensile strength of self-compacting recycled aggregate concrete.

Table 6. Summary of different model evaluation parameters of SCGB algorithm.

Step	Function	MSE	R
Training	trainscg	0.4588	0.6920
Validation	trainscg	0.5189	0.6616
Testing	trainscg	0.8925	0.5425
Overall	trainscg	0.6234	0.6368

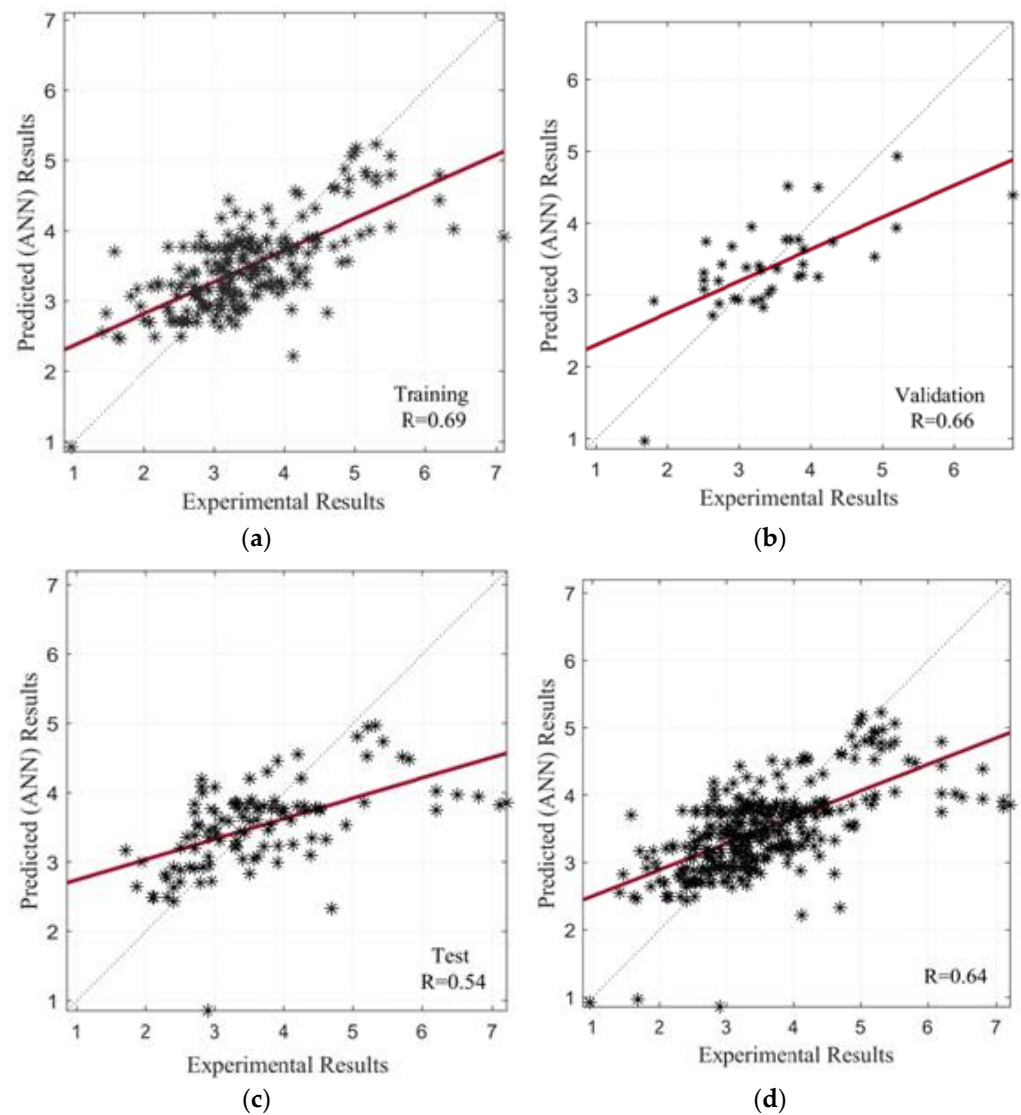
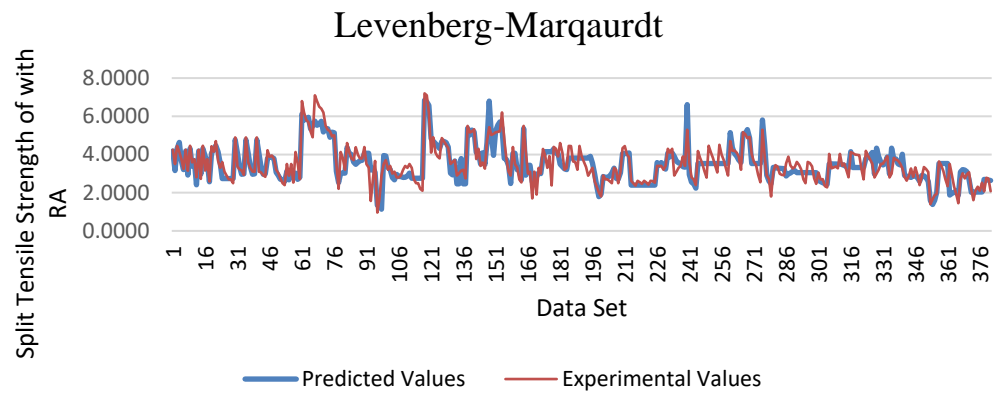


Figure 14. SCG algorithm regression graphs between the experimental and predicted tensile strength: (a) training; (b) validation; (c) testing, and (d) overall dataset.

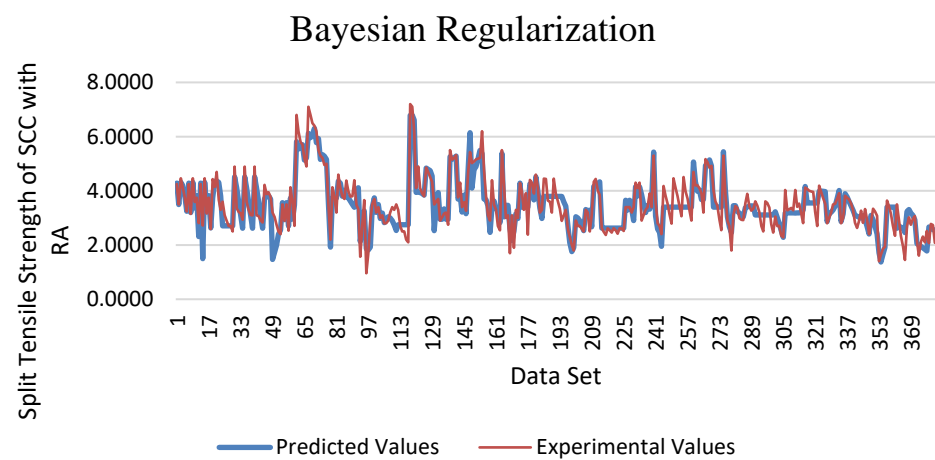
5.4. Comparison of LM and SCG Approaches

The comparison between all three algorithms was performed on the basis of the experimental results and predicted results by ANN. Figure 15a–c shows the comparison between the experimental and predicted values of a model trained by LM, BR, and SCG approaches, respectively. On the y-axis, the blue line indicates the predicted values, and the red line shows the experimental values of tensile strength of SCC with recycled aggregates. On the x-axis, the data set of 381 samples is given.

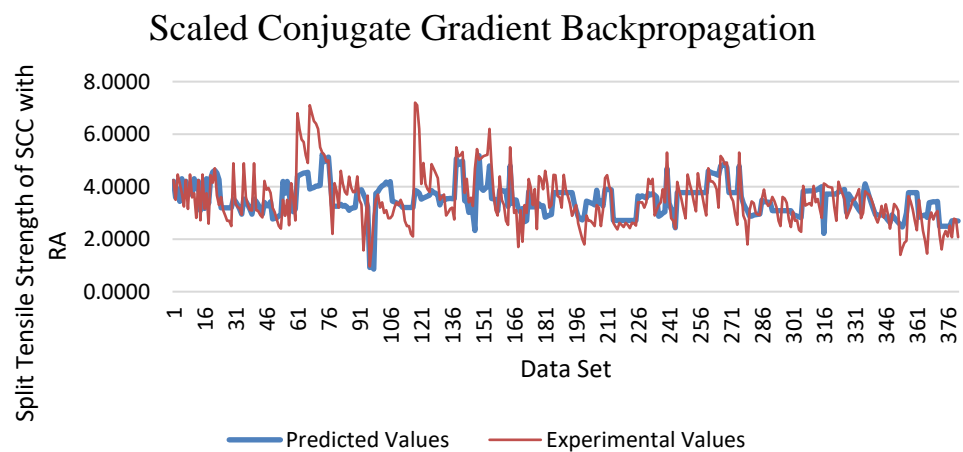
All graphs indicate that values predicted from the three algorithms correlated well with the experimental values. The more significant difference between the two lines indicates a high error between the two parameters. The overall R-value and mean squared error of all three algorithms are summarized in graphical format, as shown in Figure 16.



(a)



(b)



(c)

Figure 15. Comparison of experimental and predicted values by ANN of (a) LM, (b) BR, and (c) SCGB algorithms.

Thus, Figures 15a–c and 16 confirm that the best fitting graph is that of Bayesian regularization (Figure 15b), which has a more significant R-value and minimum MSE. The BR approach performed better because of the heterogeneity of the data, as it can provide

strong generalization for complex datasets [98]. It was concluded that among all three algorithms, i.e., Levenberg–Marquardt, Bayesian regularization, and Scaled Conjugate Gradient Backpropagation, Bayesian regularization had the highest accuracy (>90%) and could accurately predict the splitting tensile strength of self-compacting concrete with recycled aggregates.

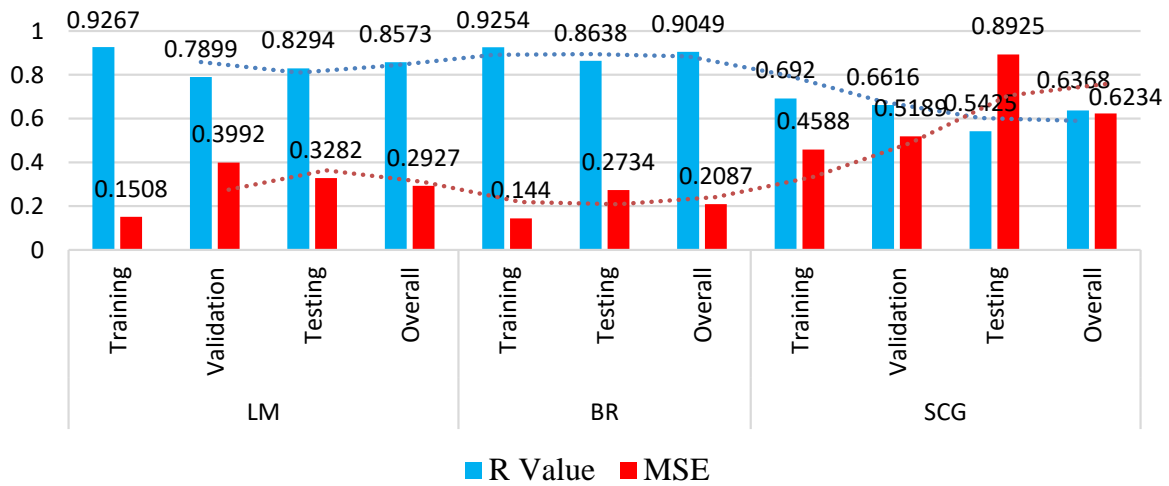


Figure 16. R-value and MSE of LM, BR, and SCGB algorithms.

5.5. Sensitivity Analysis

The sensitivity analysis allows us to see how each input variable affects the output variable. The more significant the influence of the input variables on the output variable, the higher the sensitivity values. As per Shang et al. [99], the variables of input have a significant influence on the prediction of the output variable. Sensitivity analysis was used to examine the impact of each input variable—fine-aggregate cement, coarse-aggregate superplasticizer, water, and superplasticizers—on the variability of splitting tensile strength of self-compacting concrete with recycled aggregates. Equations (2) and (3) were used to determine the sensitivity analysis:

$$S_i = \frac{N_i}{\sum_{i=1}^n N_i} \times 100 \tag{2}$$

$$N_i = f_{\max}(x_i) - f_{\min}(x_i), i = 1, \dots, n \tag{3}$$

where $f_{\max}(x_i)$ and $f_{\min}(x_i)$ are the input variables projected highest and lowest splitting tensile strength.

As indicated in the graph (Figure 17), each of the variables of input—coarse-aggregate cement, water, superplasticizers, water, fine aggregate, and mineral admixture—had a considerable impact in forecasting the splitting tensile strength of self-compacting concrete with recycled aggregates. The most significant contributions to the estimate of splitting tensile strength of self-compacting concrete with recycled aggregates were cement (30.07%), fine aggregate (22.83%), and mineral admixture (22.08%). According to Shang et al. [99], cement is a factor that significantly impacts the prediction of the tensile strength of SCC with RA. The input variables of coarse aggregate and superplasticizer had contributions of 13.02% and 9.61%, respectively. On the other hand, water was the least efficient variable in predicting the tensile strength of SCC with RA (2.39%); these findings are consistent with prior studies [98].

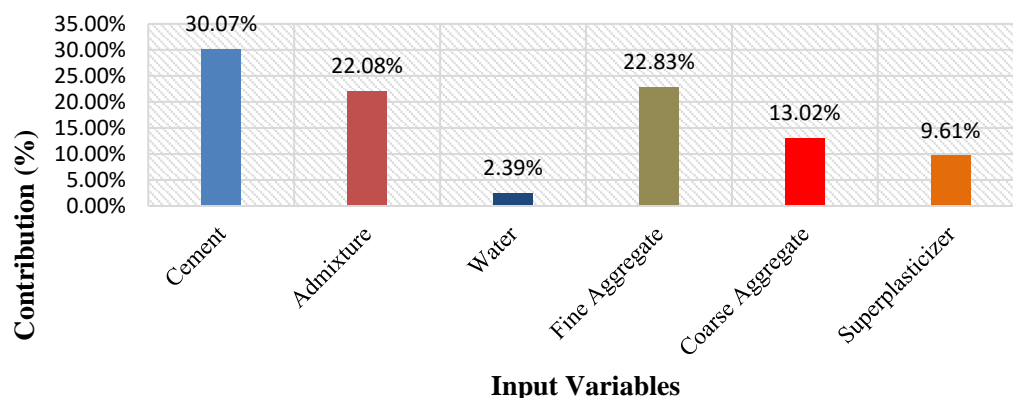


Figure 17. Contribution of input variables to split tensile strength of SSSC with RA in BR approach.

6. Conclusions

This study aimed to predict and compare the results of predicting the tensile strength of SCC modified with RA using different algorithms of artificial neural networks, namely LM, BR, and SCG. The model was trained with six input parameters: cement, water, admixtures, coarse and fine aggregates, and superplasticizer. For evaluation, two metrics were used: R-value and MSE. From this study, the following conclusions were drawn.

1. A dataset of 381 samples was collected through journals and randomly divided into 60%, 10%, and 30% for training (267), validation (38), and testing (114), respectively, for the development of the LM, BR, and SCG models. However, in the case of BR, the ratio was 70% for training and 30% for testing due to the built-in validation function in the training step.
2. Different algorithms, namely LM, BR, and SCG, were trained and tested for this study and gave an overall accuracy of 85%, 91%, and 64% with MSEs of 0.2927, 0.2087, and 0.6234.
3. It is evident that out of all three, the SCG algorithm was a poor model for predicting the tensile strength of SCC, with RA having the lowest R-value and the highest MSE.
4. Bayesian regularization gave the best performance with a high coefficient of correlation ($R > 90\%$) and a minimal MSE (0.2087) concerning LM and SCG.
5. The results showed that the BR algorithm is a good model and can be adopted for the prediction of the 28-day tensile strength of self-compacting concrete modified with recycled aggregates.
6. According to the sensitivity analysis, cement is the essential input variable in predicting the 28-day tensile strength of SCC with RA (30.07%). On the other hand, water had the smallest influence on the 28-day tensile strength of SCC with RA (2.39%).

There are some limitations in this research regarding the collection of data. As there were not enough experimental data, we could not gather large datasets for this research. As a result, more datasets must be collected for future research on this topic to avoid this limitation and make a more accurate prediction model. With more data, various inputs and outputs can be further examined.

Author Contributions: Conceptualization, J.d.-P.-G.; investigation, J.d.-P.-G., O.Z. and R.M.-G.; writing—original draft preparation, J.d.-P.-G., O.Z. and R.M.-G.; writing—review and editing, J.d.-P.-G., C.P., O.Z. and R.M.-G.; supervision, C.P. and R.M.-G. All authors have read and agreed to the published version of the manuscript.

Funding: This research received no external funding.

Institutional Review Board Statement: Not applicable.

Informed Consent Statement: Not applicable.

Data Availability Statement: Data is accessible from the corresponding author on reasonable request.

Conflicts of Interest: The authors declare no conflict of interest.

References

1. Bilim, C.; Atiş, C.; Tanyildizi, H.; Karahan, O. Predicting the compressive strength of ground granulated blast furnace slag concrete using artificial neural network. *Adv. Eng. Softw.* **2009**, *40*, 334–340. [CrossRef]
2. Li, Z. *Advanced Concrete Technology*; John Willey & Sons: Toronto, ON, Canada, 2011.
3. Saidova, Z.; Yakovlev, G.; Smirnova, O.; Gordina, A.; Kuzmina, N. Modification of cement matrix with complex additive based on chrysotyl nanofibers and carbon black. *Appl. Sci.* **2021**, *11*, 6943. [CrossRef]
4. Okamura, H.; Ouchi, M. Self-compacting concrete. *J. Adv. Concr. Technol.* **2003**, *1*, 5–15. [CrossRef]
5. Zaid, O.; Hashmi, S.R.Z.; Aslam, F.; Abedin, Z.U.; Ullah, A. Experimental study on the properties improvement of hybrid graphene oxide fiber-reinforced composite concrete. *Diam. Relat. Mater.* **2022**, *124*, 108883. [CrossRef]
6. Zaid, O.; Ahmad, J.; Siddique, M.S.; Aslam, F.; Alabduljabbar, H.; Khedher, K.M. A step towards sustainable glass fiber reinforced concrete utilizing silica fume and waste coconut shell aggregate. *Sci. Rep.* **2021**, *11*, 1–14. Available online: <https://www.nature.com/articles/s41598-021-92228-6> (accessed on 22 June 2022).
7. Zaid, O.; Mukhtar, F.M.; M-García, R.; El Sherbiny, M.G.; Mohamed, A.M. Characteristics of high-performance steel fiber reinforced recycled aggregate concrete utilizing mineral filler. *Case Stud. Constr. Mater.* **2022**, *16*, e00939. [CrossRef]
8. Yakovlev, G.; Polyanskikh, I.; Gordina, A.; Pudov, I.; Černý, V.; Gumenyuk, A.; Smirnova, O. Influence of sulphate attack on properties of modified cement composites. *Appl. Sci.* **2021**, *11*, 8509. [CrossRef]
9. Smirnova, O.M.; de Navascués, I.M.P.; Mikhailevskii, V.R.; Kolosov, O.I.; Skolota, N.S. Sound-absorbing composites with rubber crumb from used tires. *Appl. Sci.* **2021**, *11*, 7347. [CrossRef]
10. Shi, C.; Wu, Z.; Lv, K.; Wu, L. A review on mixture design methods for self-compacting concrete. *Constr. Build. Mater.* **2015**, *84*, 387–398. [CrossRef]
11. Smirnova, O.; Kazanskaya, L.; Koplík, J.; Tan, H.; Gu, X. Sustainability, and undefined 2020, Concrete based on clinker-free cement: Selecting the functional unit for environmental assessment. *Sustainability* **2021**, *13*, 135. [CrossRef]
12. Smirnova, O. Development of classification of rheologically active microfillers for disperse systems with Portland cement and superplasticizer. *Int. J. Civ. Eng. Technol.* **2018**, *9*, 1966–1973.
13. Nikbin, I.M.; Beygi, M.H.A.; Kazemi, M.T.; Vaseghi Amiri, J.; Rabbanifar, S.; Rahmani, E.; Rahimi, S. A comprehensive investigation into the effect of water to cement ratio and powder content on mechanical properties of self-compacting concrete. *Constr. Build. Mater.* **2014**, *57*, 69–80. [CrossRef]
14. Althoey, F.; Zaid, O.; De-Prado-Gil, J.; Palencia, C.; Ali, E.; Hakeem, I.; Martínez-García, R. Impact of sulfate activation of rice husk ash on the performance of high strength steel fiber reinforced recycled aggregate concrete. *J. Build. Eng.* **2022**, *54*, 104610. [CrossRef]
15. Zaid, O.; Ahmad, J.; Siddique, M.S.; Aslam, F. Effect of Incorporation of Rice Husk Ash Instead of Cement on the Performance of Steel Fibers Reinforced Concrete. *Front. Mater.* **2021**, *8*, 151. [CrossRef]
16. Tam, V.W.Y.; Shen, L.Y.; Fung, I.W.H.; Wang, J.Y. Controlling construction waste by implementing governmental ordinances in Hong Kong. *Constr. Innov.* **2007**, *7*, 149–166. [CrossRef]
17. Borrero, E.L.S.; Farhangi, V.; Jadidi, K.; Karakouzian, M. An Experimental Study on Concrete's Durability and Mechanical Characteristics Subjected to Different Curing Regimes. *Civ. Eng. J.* **2021**, *7*, 676–689. [CrossRef]
18. Huang, X.; Ge, J.; Kaewunruen, S.; Su, Q. The self-sealing capacity of environmentally friendly, highly damped, fibre-reinforced concrete. *Materials* **2020**, *13*, 298. [CrossRef]
19. Daungwilailuk, T.; Cao, T.; Pansuk, W.; Pheinsusom, P. Evaluating damaged concrete depth in reinforced concrete structures under different fire exposure times by means of NDT and DT techniques. *Mod. Eng. Technol.* **2017**, *21*, 233–249. [CrossRef]
20. Jiradilok, P.; Wang, Y.; Nagai, K.; Matsumoto, K. Development of discrete meso-scale bond model for corrosion damage at steel-concrete interface based on tests with/without concrete damage. *Constr. Build. Mater.* **2020**, *263*, 117615. [CrossRef]
21. Aslam, F.; Zaid, O.; Althoey, F.; Alyami, S.H.; Qaidi, S.; Gil, J.D.P.; Martínez-García, R. Evaluating the influence of fly ash and waste glass on the characteristics of coconut fibers reinforced concrete. *Struct. Concr.* **2022**. [CrossRef]
22. Ahmad, J.; Zaid, O.; Aslam, F.; Shahzaib, M.; Ullah, R.; Alabduljabbar, H.; Khedher, K.M. A study on the mechanical characteristics of glass and nylon fiber reinforced peach shell lightweight concrete. *Materials* **2021**, *14*, 4488. [CrossRef] [PubMed]
23. Smirnova, O.M.; Pidal, I.M.; Alekseev, A.V.; Petrov, D.N.; Popov, M.G. Strain Hardening of Polypropylene Microfiber Reinforced Composite Based on Alkali-Activated Slag Matrix. *Materials* **2022**, *15*, 1607. [CrossRef] [PubMed]
24. Carvalho, F.P. Mining industry and sustainable development: Time for change. *Food Energy Secur.* **2017**, *6*, 61–77. [CrossRef]
25. Zaid, O.; Martínez-García, R.; Abadel, A.A.; Fraile-Fernández, F.J.; Alshaiikh, I.M.H.; Palencia-Coto, C. To determine the performance of metakaolin-based fiber-reinforced geopolymer concrete with recycled aggregates. *Arch. Civ. Mech. Eng.* **2022**, *22*, 1–14. [CrossRef]
26. Zaid, O.; Hashmi, S.R.Z.; Aslam, F.; Alabduljabbar, H. Experimental Study on Mechanical Performance of Recycled Fine Aggregate Concrete Reinforced With Discarded Carbon Fibers. *Front. Mater.* **2021**, *8*, 771423. [CrossRef]
27. Kaewunruen, S.; Meesit, R. Eco-friendly High-Strength Concrete Engineering by Micro Crumb Rubber from Recycled Tires and Plastic Components. *Adv. Civ. Eng.* **2020**, *9*, 210–226. [CrossRef]
28. Smirnova, O.M. Low-clinker cements with low water demand. *J. Mater. Civ. Eng.* **2020**, *32*, 06020008. [CrossRef]

29. Smirnova, O.J. Compatibility of shungisite microfillers with polycarboxylate admixtures in cement compositions. *Eng. Appl. Sci.* **2019**, *14*, 600–610. Available online: http://www.arnjournals.org/jeas/research_papers/rp_2019/jeas_0219_7595.pdf (accessed on 22 June 2022).
30. Nguyen, H.Y.T.; Pansuk, W.; Sanchaoren, P. The Effects of Electro-Chemical Chloride Extraction on the Migration of Ions and the Corrosion State of Embedded Steel in Reinforced Concrete. *KSCE J. Civ. Eng.* **2018**, *22*, 2942–2950. [[CrossRef](#)]
31. Berndt, M.L. Properties of sustainable concrete containing fly ash, slag and recycled concrete aggregate. *Constr. Build. Mater.* **2009**, *23*, 2606–2613. [[CrossRef](#)]
32. Nikoo, M.; Torabian Moghadam, F.; Sadowski, L. Prediction of concrete compressive strength by evolutionary artificial neural networks. *Adv. Mater. Sci. Eng.* **2015**, *2015*, 849126. [[CrossRef](#)]
33. Dabiri, H.; Farhangi, V.; Moradi, M.J.; Zadehmohamad, M.; Karakouzian, M. Applications of Decision Tree and Random Forest as Tree-Based Machine Learning Techniques for Analyzing the Ultimate Strain of Spliced and Non-Spliced Reinforcement Bars. *Appl. Sci.* **2022**, *12*, 4851. [[CrossRef](#)]
34. Du, X.; Cai, Y.; Wang, S.; Zhang, L. Overview of deep learning. In Proceedings of the 2016 31st Youth Academic Annual Conference of Chinese Association of Automation (YAC), Wuhan, China, 11–13 November 2016; pp. 159–164.
35. Schmidhuber, J. Deep learning in neural networks: An overview. *Neural Netw.* **2015**, *61*, 85–117. [[CrossRef](#)]
36. Levenberg, K. A method for the solution of certain non-linear problems in least squares. *Q. Appl. Math.* **1944**, *2*, 164–168. [[CrossRef](#)]
37. Marquardt, D.W. An algorithm for least-squares estimation of nonlinear parameters. *J. Soc. Ind. Appl. Math.* **1963**, *11*, 431–441. [[CrossRef](#)]
38. Mittelmann, H.D. The Least Squares Problem. 2004. Available online: <http://plato.asu.edu/topics/problems/nlolsq> (accessed on 22 June 2022).
39. Madsen, K.; Nielsen, H.B.; Tingleff, O. *Methods for Non-Linear Least Squares Problems*, 2nd ed.; Elsevier: Aalborg, Denmark, 2008.
40. MacKay, D.J.C. Bayesian Interpolation. *Neural Comput.* **1992**, *4*, 415–447. [[CrossRef](#)]
41. Winkler, D.A.; Burden, F.R. Robust QSAR models from novel descriptors and bayesian regularised neural networks. *Mol. Simul.* **2000**, *24*, 243–258. [[CrossRef](#)]
42. Hawkins, D.M.; Basak, S.C.; Mills, D. Assessing Model Fit by Cross-Validation. *J. Chem. Inf. Comput. Sci.* **2003**, *43*, 579–586. [[CrossRef](#)]
43. Lucic, B.; Amic, D.; Trinajstic, N. Nonlinear multivariate regression outperforms several concisely designed neural networks on three QSPR data sets. *J. Chem. Inf. Comput. Sci.* **2000**, *40*, 403–413. [[CrossRef](#)]
44. Hagan, M.T.; Demuth, H.B.; de Jesús, O. An introduction to the use of neural networks in control systems. *Int. J. Robust Nonlinear Control.* **2002**, *12*, 959–985. [[CrossRef](#)]
45. Kişi, Ö.; Uncuoğlu, E. Comparison of three back-propagation training algorithms for two case studies. *Indian J. Eng. Mater. Sci.* **2005**, *12*, 434–442.
46. Demuth, H.; Beale, M.; Hagan, M. *Neural Network Toolbox 6. User's Guide*; The MathWorks: Natick, MA, USA, 2010.
47. Møller, M.F. A scaled conjugate gradient algorithm for fast supervised learning. *Neural Netw.* **1993**, *6*, 525–533. [[CrossRef](#)]
48. Ali, E.; Al-Tersawy, S.H. Recycled glass as a partial replacement for fine aggregate in self compacting concrete. *Constr. Build. Mater.* **2012**, *35*, 785–791. [[CrossRef](#)]
49. Nieto, D.; Dapena, E.; Alaejos, P.; Olmedo, J.; Pérez, D. Properties of Self-Compacting Concrete Prepared with Coarse Recycled Concrete Aggregates and Different Water: Cement Ratios. *J. Mater. Civ. Eng.* **2018**, *31*, 04018376. [[CrossRef](#)]
50. Aslani, F.; Ma, G.; Yim Wan, D.L.; Muselin, G. Development of high-performance self-compacting concrete using waste recycled concrete aggregates and rubber granules. *J. Clean. Prod.* **2018**, *182*, 553–556. [[CrossRef](#)]
51. Nili, M.; Sasanipour, H.; Aslani, F. The Effect of Fine and Coarse Recycled Aggregates on Fresh and Mechanical Properties of Self-Compacting Concrete. *Materials* **2019**, *12*, 1120. [[CrossRef](#)]
52. Babalola, E.; Awoyera, P.O.; Tran, M.T.; Le, D.-H.; Olalusi, O.B.; Vilaria, A.; Ovallos-Gazabon, D. Mechanical and durability properties of recycled aggregate concrete with ternary binder system and optimized mix proportion. *J. Mater. Res. Technol.* **2020**, *9*, 6521–6532. [[CrossRef](#)]
53. Pan, Z.; Zhou, J.; Jiang, X.; Xu, Y.; Jin, R.; Mas, J.; Zhuang, Y.; Diao, Z.; Zhang, S.; Si, Q.; et al. Investigating the effects of steel slag powder on the properties of self-compacting concrete with recycled aggregates. *Constr. Build. Mater.* **2019**, *200*, 570–577. [[CrossRef](#)]
54. Bahrami, N.; Zohrabi, M.; Mahmoudy, S.A.; Akbari, M. Optimum recycled concrete aggregate and micro-silica content in self-compacting concrete: Rheological, mechanical and microstructural properties. *J. Build. Eng.* **2021**, *31*, 101361. [[CrossRef](#)]
55. Revathi, P.; Selvi, R.; Velin, S.S. Investigations on Fresh and Hardened Properties of Recycled Aggregate Self Compacting Concrete. *J. Inst. Eng. (India) Ser. A* **2013**, *94*, 179–185. [[CrossRef](#)]
56. Behera, M.; Minocha, A.K.; Bhattacharyya, S.K. Flow behavior, microstructure, strength and shrinkage properties of self-compacting concrete incorporating recycled fine aggregate. *Constr. Build. Mater.* **2019**, *228*, 116819. [[CrossRef](#)]
57. Revilla-Cuesta, V.; Ortega-López, V.; Skaf, M.; Manso, J.M. Effect of fine recycled concrete aggregate on the mechanical behavior of self-compacting concrete. *Constr. Build. Mater.* **2020**, *263*, 120671. [[CrossRef](#)]
58. Chakkamalayath, J.; Joseph, A.; Al-Baghli, H.; Hamadah, O.; Dashti, D.; Abdulmalek, N. Performance evaluation of self-compacting concrete containing volcanic ash and recycled coarse aggregates. *Asian J. Civ. Eng.* **2020**, *21*, 815–827. [[CrossRef](#)]

59. Sadeghi-Nik, A.; Berenjian, J.; Alimohammadi, S.; Lotfi-Omran, O.; Sadeghi-Nik, A.; Karimaei, M. The Effect of Recycled Concrete Aggregates and Metakaolin on the Mechanical Properties of Self-Compacting Concrete Containing Nanoparticles. *Iran. J. Sci. Technol. Trans. Civ. Eng.* **2018**, *43*, 503–515. [[CrossRef](#)]
60. Duan, Z.; Singh, A.; Xiao, J.; Hou, S. Combined use of recycled powder and recycled coarse aggregate derived from construction and demolition waste in self-compacting concrete. *Constr. Build. Mater.* **2020**, *254*, 119323. [[CrossRef](#)]
61. Señas, L.; Priano, C.; Marfil, S. Influence of recycled aggregates on properties of self-consolidating concretes. *Constr. Build. Mater.* **2016**, *113*, 498–505. [[CrossRef](#)]
62. Fiol, F.; Thomas, C.; Muñoz, C.; Ortega-López, V.; Manso, J.M. The influence of recycled aggregates from precast elements on the mechanical properties of structural self-compacting concrete. *Constr. Build. Mater.* **2018**, *182*, 309–323. [[CrossRef](#)]
63. Sharafi, Y.; Houshiar, M.; Aghebati, B. Recycled glass replacement as fine aggregate in self-compacting concrete. *Front. Struct. Civ. Eng.* **2013**, *7*, 419–428. [[CrossRef](#)]
64. Martínez-García, R.; Guerra-Romero, I.M.; Morán-del Pozo, J.M.; de Brito, J.; Juan-Valdés, A. Recycling Aggregates for Self-Compacting Concrete Production: A Feasible Option. *Materials* **2020**, *13*, 868. [[CrossRef](#)]
65. Khafaga, S.A. Production of high strength self compacting concrete using recycled concrete as fine and/or coarse aggregates. *World Appl. Sci. J.* **2014**, *29*, 465–474. Available online: <https://www.idosi.org/wasj/wasj2914/1.pdf> (accessed on 22 June 2022).
66. Gesoglu, M.; Güneysi, E.; Öz, H.Ö.; Taha, I.; Yasemin, M.T. Failure characteristics of self-compacting concretes made with recycled aggregates. *Constr. Build. Mater.* **2015**, *98*, 334–344. [[CrossRef](#)]
67. Silva, Y.F.; Robayo, R.A.; Matthey, P.; Delvasto, S. Properties of self-compacting concrete on fresh and hardened with residue of masonry and recycled concrete. *Constr. Build. Mater.* **2016**, *124*, 639–644. [[CrossRef](#)]
68. Grdic, D.; Ristic, N.; Toplicic-Curcic, G.; Krstic, D. Potential of usage of self-compacting concrete with addition of recycled CRT glass for production of precast concrete elements. *Facta Univ.-Ser. Archit. Civ. Eng.* **2018**, *16*, 57–66. [[CrossRef](#)]
69. Singh, A.; Duan, Z.; Xiao, J.; Liu, Q. Incorporating recycled aggregates in self-compacting concrete: A review. *J. Sustain. Cem.-Based Mater.* **2019**, *9*, 165–189. [[CrossRef](#)]
70. Güneysi, E.; Gesoğlu, M.; Algin, Z.; Yazici, H. Effect of surface treatment methods on the properties of self-compacting concrete with recycled aggregates. *Constr. Build. Mater.* **2014**, *64*, 172–183. [[CrossRef](#)]
71. Sun, C.; Chen, Q.; Xiao, J.; Liu, W. Utilization of waste concrete recycling materials in self-compacting concrete. *Resour. Conserv. Recycl.* **2020**, *161*, 104930. [[CrossRef](#)]
72. Guo, Z.; Jiang, T.; Zhang, J.; Kong, X.; Chen, C.; Lehman, D. E Mechanical and durability properties of sustainable self-compacting concrete with recycled concrete aggregate and fly ash, slag and silica fume. *Constr. Build. Mater.* **2020**, *231*, 117115. [[CrossRef](#)]
73. Surendar, M.; Gnana Ananthi, G.; Sharaniya, M.; Deepak, M.S.; Soundarya, T.V. Mechanical properties of concrete with recycled aggregate and M–sand. *Mater. Today Proc.* **2021**, *44*, 1723–1730. [[CrossRef](#)]
74. Katar, I.; Ibrahim, Y.; Abdul Malik, M.; Khahro, S.H. Mechanical Properties of Concrete with Recycled Concrete Aggregate and Fly Ash. *Recycling* **2021**, *6*, 23. [[CrossRef](#)]
75. Tang, W.C.; Ryan, P.C.; Cui, H.; Liao, W. Properties of Self-Compacting Concrete with Recycled Coarse Aggregate. *Adv. Mater. Sci. Eng.* **2016**, *2016*, 1–11. [[CrossRef](#)]
76. Khodair, Y.; Luqman. Self-compacting concrete using recycled asphalt pavement and recycled concrete aggregate. *J. Build. Eng.* **2017**, *12*, 282–287. [[CrossRef](#)]
77. Thienpont, T.; de Corte, W.; Seitl, S. Self-compacting Concrete, Protecting Steel Reinforcement under Cyclic Load: Evaluation of Fatigue Crack Behavior. *Procedia Eng.* **2016**, *160*, 207–213. [[CrossRef](#)]
78. Kou, S.C.; Poon, C.S. Properties of self-compacting concrete prepared with recycled glass aggregate. *Cem. Concr. Compos.* **2009**, *31*, 107–113. [[CrossRef](#)]
79. Tuyan, M.; Mardani-Aghabaglou, A.; Ramyar, K. Freeze–thaw resistance, mechanical and transport properties of self-consolidating concrete incorporating coarse recycled concrete aggregate. *Mater. Des.* **2014**, *53*, 983–991. [[CrossRef](#)]
80. Siva, S.; Krishna, R.; Sowjanya Vani, V.; Khader, S.; Baba, V. Studies on Mechanical Properties of Ternary Blended Self-Compacting Concrete Using Different Percentages of Recycled Aggregate. *Int. J. Civ. Eng. Technol. (IJCIET)* **2018**, *9*, 1672–1680. [[CrossRef](#)]
81. Uygunoğlu, T.; Topçu, I.B.; Çelik, A.G. Use of waste marble and recycled aggregates in self-compacting concrete for environmental sustainability. *J. Clean. Prod.* **2014**, *84*, 691–700. [[CrossRef](#)]
82. Vinay Kumar, B.M.; Ananthan, H.; Balaji, K.V.A. Experimental studies on utilization of coarse and finer fractions of recycled concrete aggregates in self compacting concrete mixes. *J. Build. Eng.* **2017**, *9*, 100–108. [[CrossRef](#)]
83. Wang, J.; Dai, Q.; Si, R.; Ma, Y.; Guo, S. Fresh and mechanical performance and freeze-thaw durability of steel fiber-reinforced rubber self-compacting concrete (SRSCC). *J. Clean. Prod.* **2020**, *277*, 123180. [[CrossRef](#)]
84. Long, W.; Shi, J.; Wang, W.; Fang, X. Shrinkage of Hybrid Fiber Reinforced Self-Consolidating Concrete with Recycled Aggregate. In *Flowing Towards Sustainability, Proceedings of the SCC-2016 8th International RILEM Symposium on Self-Compacting Concrete, Washington, DC, USA, 15–18 May 2016*; Khayat, K.H., Ed.; RILEM: Paris, France, 2016; pp. 751–762.
85. Yu, T.; Fang, L.; Teng, J.G. FRP-Confined Self-Compacting Concrete under Axial Compression. *J. Mater. Civ. Eng.* **2014**, *26*, 04014082. [[CrossRef](#)]
86. Mahakavi, P.; Chithra, R. Effect of recycled coarse aggregate and manufactured sand in self compacting concrete. *Aust. J. Struct. Eng.* **2019**, *21*, 33–43. [[CrossRef](#)]

87. Chen, X.; Wu, S.; Zhou, J. Quantification of dynamic tensile behavior of cement-based materials. *Constr. Build. Mater.* **2014**, *51*, 15–23. [[CrossRef](#)]
88. Manzi, S.; Mazzotti, C.; Bignozzi, M.C. Self-compacting concrete with recycled concrete aggregate: Study of the long-term properties. *Constr. Build. Mater.* **2017**, *157*, 582–590. [[CrossRef](#)]
89. Rathakrishnan, V.; Beddu, S.; Ahmed, A. Comparison studies between machine learning optimisation technique on predicting concrete compressive strength. *Res. Square* **2021**. [[CrossRef](#)]
90. Hassan, A.N.; El-Hag, A. Two-Layer Ensemble-Based Soft Voting Classifier for Transformer Oil Interfacial Tension Prediction. *Energies* **2020**, *13*, 1735. [[CrossRef](#)]
91. Koya, B.P. Comparison of Different Machine Learning Algorithms to Predict Mechanical Properties of Concrete. Master's Thesis, University of Victoria, Victoria, Canada, 2021. Available online: <http://hdl.handle.net/1828/12574> (accessed on 29 May 2022).
92. Khademi, F.; Jamal, S.; Deshpande, N.; Londhe, S. Predicting strength of recycled aggregate concrete using artificial neural network, adaptive neuro-fuzzy inference system and multiple linear regression. *Int. J. Sustain. Built Environ.* **2016**, *5*, 355–369. [[CrossRef](#)]
93. Uysal, M.; Tanyildizi, H. Predicting the core compressive strength of self-compacting concrete (SCC) mixtures with mineral additives using artificial neural network. *Constr. Build. Mater.* **2011**, *25*, 4105–4111. [[CrossRef](#)]
94. Hanbay, D.; Turkoglu, I.; Demir, Y. Prediction of wastewater treatment plant performance based on wavelet packet decomposition and neural networks. *Expert Syst. Appl.* **2008**, *34*, 1038–1043. [[CrossRef](#)]
95. Baghirli, O. Comparison of Lavenberg-Marquardt, Scaled Conjugate Gradient and Bayesian Regularization Backpropagation Algorithms for Multistep Ahead Wind Speed Forecasting Using Multilayer Perceptron Feedforward Neural Network. Master's Thesis, Uppsala University, Uppsala, Sweden, 2015. Available online: <https://www.diva-portal.org/smash/record.jsf?pid=diva2%3A828170&dswid=6956> (accessed on 29 May 2022).
96. Babajanzadeh, M.; Azizifar, V. Compressive strength prediction of self-compacting concrete incorporating silica fume using artificial intelligence methods. *Civ. Eng. J.* **2018**, *4*, 1542.
97. Olu-Ajayi, R.; Alaka, H.; Sulaimon, I.; Sunmola, F.; Ajayi, S. Building energy consumption prediction for residential buildings using deep learning and other machine learning techniques. *J. Build. Eng.* **2022**, *45*, 103406. [[CrossRef](#)]
98. Suescum-Morales, D.; Salas-Morera, L.; Ramón Jiménez, J.; García-Hernández, L. A Novel Artificial Neural Network to Predict Compressive Strength of Recycled Aggregate Concrete. *Appl. Sci.* **2021**, *11*, 11077. [[CrossRef](#)]
99. Shang, M.; Li, H.; Ahmad, A.; Ahmad, W.; Ostrowski, K.; Aslam, F.; Joyklad, P.; Majka, T.M. Predicting the Mechanical Properties of RCA-Based Concrete Using Supervised Machine Learning Algorithms. *Materials* **2022**, *15*, 647. [[CrossRef](#)] [[PubMed](#)]